

Synthesis of *n*-Butylamine from Butyronitrile on Ni/SiO₂: Effect of Solvent

Darío J. Segobia, Andrés F. Trasarti and Carlos R. Apesteguía*

Catalysis Science and Engineering Research Group (GICIC), INCAPE, UNL-CONICET,
Santiago del Estero 2654, (3000) Santa Fe, Argentina

O efeito de solvente sobre a atividade e seletividade de Ni(10.5%)/SiO₂ no processo de hidrogenação em fase líquida da butironitrila a butilaminas foi estudado a 373 K e 13 bar usando-se etanol, benzeno, tolueno e ciclohexano como solventes. Em etanol, um solvente prótico, o catalisador de Ni produziu *n*-butilamina (84%) e dibutilamina (16%). Quando solventes apolares, tais como ciclohexano, tolueno ou benzeno, foram usados, a força de interação solvente-catalisador determinou a seletividade para formação de *n*-butilamina: quanto mais forte a interação solvente-catalisador, maior era a produção de *n*-butilamina. O rendimento de *n*-butilamina em solventes apolares variou entre 39% (ciclohexano) e 63% (benzeno).

The effect of solvent on Ni(10.5%)/SiO₂ activity and selectivity for the liquid-phase hydrogenation of butyronitrile to butylamines was studied at 373 K and 13 bar using ethanol, benzene, toluene and cyclohexane as solvents. In ethanol, a protic solvent, the Ni catalyst yielded *n*-butylamine (84%) and dibutylamine (16%). When non-polar solvents, such as cyclohexane, toluene or benzene, were used, the solvent-catalyst interaction strength determined the selectivity to *n*-butylamine: the stronger the solvent-catalyst interaction the higher the *n*-butylamine production. The yield to *n*-butylamine in non-polar solvents varied between 39% (cyclohexane) and 63% (benzene).

Keywords: butyronitrile, butylamines, selective hydrogenation, Ni catalysts

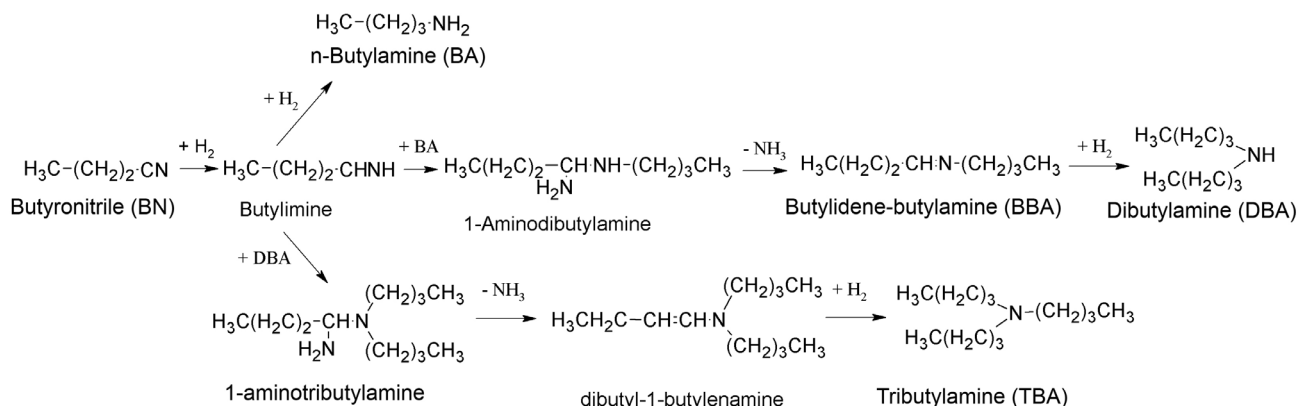
Introduction

The hydrogenation of nitriles is used to produce primary amines that are valuable raw materials for obtaining many chemicals, pharmaceuticals and polymers.¹ At industrial level, the reaction is performed over transition metal catalysts at high hydrogen pressures. Nevertheless, nitrile hydrogenation usually proceeds stepwise via consecutive condensation/hydrogenation reactions that finally form a mixture of ammonia and primary, secondary, and tertiary amines. In order to obtain selectively primary amines, the formation of secondary and tertiary amines has to be avoided. In previous works, large amounts of ammonia have often been employed to suppress the formation of higher amines, since ammonia is released in condensation reactions leading to higher amines.^{2,3} However, the addition of ammonia creates waste problems that make the process more expensive, and less easy to implement on an industrial scale. Thus, there is a need to develop stable and selective metal-supported catalysts for hydrogenating nitriles to primary amines under mild operation conditions.

The mechanism of nitrile hydrogenation and condensation to higher amines accepted by many authors is based on the pioneer work of Sabatier and Senderens,⁴ Von Braun *et al.*,⁵ and others.^{6,7} This mechanism is depicted in Scheme 1 for butyronitrile (BN) hydrogenation to *n*-butylamine (BA) and coupling reactions leading to dibutylamine (DBA) and tributylamine (TBA).^{8,9} Based on the proposal of Von Braun *et al.*,⁵ Scheme 1 includes the initial hydrogenation of butyronitrile to butylimine that is consecutively hydrogenated to *n*-butylamine. Butylimine is a highly reactive aldimine intermediate that interacts with *n*-butylamine to form 1-aminodibutylamine. This latter intermediate gives by deamination the secondary imine, butylidene-butylamine (BBA), that is further hydrogenated to dibutylamine. Similarly, butylimine may react with dibutylamine giving 1-aminotributylamine that after consecutive deamination and hydrogenation leads to the formation of tributylamine.

There is a general agreement that on metal-supported catalysts the reaction selectivity depends mainly on the nature of the metal component.^{10,11} It has been reported that Ni, Co and Ru form predominantly primary amines while Rh, Pt and Pd promote the formation of secondary

*e-mail: capesteg@fiq.unl.edu.ar



Scheme 1. Reaction network of butyronitrile hydrogenation and coupling to amines.

and tertiary amines.^{12,13} Raney Co and Ni catalysts have been extensively employed to yield primary amines by liquid-phase nitrile hydrogenation.^{12,14-16} Supported Co and Ni catalysts have been also studied in an attempt to overcome the difficulties of handling skeletal catalysts.^{8,11,17-19} Nevertheless, the reaction selectivity depends also on other parameters such as the support acid/base properties, the operation conditions and the nature of the solvent. In particular, the influence of the solvent has been little investigated, even though the choice of suitable solvents is frequently critical to obtain high catalytic activity and selectivity.²⁰⁻²² In particular, butyronitrile hydrogenation has been studied using different solvents such as methanol, ethanol, ethyl acetate, hexane, heptane and octane, and also under solvent-free conditions.^{7,8,10,11,13,15}

In this work we studied the liquid-phase hydrogenation of butyronitrile on Ni/SiO₂ in ethanol (protic solvent), cyclohexane (non-polar naphthenic solvent), and toluene and benzene (non-polar aromatic solvents). The goal was to establish the solvent effect on the catalyst activity and selectivity for promoting the synthesis of *n*-butylamine. In recent works we have discussed the influence that the solvent-catalyst, solvent-reactant and reactant-solvent-catalyst interactions have on the activity and selectivity of metal-supported catalysts for liquid-phase hydrogenation reactions.²³⁻²⁵ Here, the results will show that Ni/SiO₂ activity and selectivity for BN hydrogenation greatly depend on the solvent nature. Results are interpreted by relating the catalyst performance with both the solvent-BA interaction and the solvent-catalyst interaction strength.

Experimental

Catalyst preparation and characterization

Ni(10.5%)/SiO₂ catalyst was prepared by impregnating Ni(NO₃)₂·6H₂O (Fluka, 98%) on a commercial SiO₂

powder (Sigma-Aldrich, G62, 60-200 mesh, 300 m² g⁻¹) by incipient-wetness impregnation at 303 K. The impregnated sample was dried overnight at 373 K, then heated in air at 5 K min⁻¹ to 673 K and kept at this temperature for 2 h.

Brunauer-Emmett-Teller (BET) surface areas were measured by N₂ physisorption at its boiling point in a Micromeritics Accusorb 2100E sorptometer. Elemental compositions were measured by inductively coupled plasma atomic emission spectroscopy (ICP-AES), using a Perkin-Elmer Optima 2100 unit. Powder X-ray diffraction (XRD) patterns were collected in the range of 2θ = 10-70° using a Shimadzu XD-D1 diffractometer and Ni-filtered Cu Kα radiation.

Metal dispersion (D_{Ni}, surface Ni atoms / total M atoms) was determined by chemisorption of hydrogen. Volumetric adsorption experiments were performed at 298 K in a conventional vacuum unit. Catalysts were reduced in H₂ at 673 K for 2 h and then outgassed 2 h at 673 K prior to performing gas chemisorption experiments. Hydrogen uptake was determined using the double isotherm method as detailed in a previous work.²⁶ A stoichiometric atomic ratio of H/Ni_s = 1, where Ni_s implies a metal atom on surface, was used to calculate the metal dispersion.

Temperature programmed reduction (TPR) experiments were performed in a Micromeritics AutoChem II 2920, using 5% H₂/Ar gaseous mixture at 60 mL min⁻¹ standard temperature and pressure (STP) conditions. The sample size was 150 mg. Samples were heated from 298 to 973 K at 10 K min⁻¹. Since water is formed during sample reduction, the gas exiting from the reactor was passed through a cold trap before entering the thermal conductivity detector.

Temperature-programmed desorption experiments

The solvent interactions with the Ni/SiO₂ catalyst were studied by temperature-programmed desorption (TPD) of the solvent preadsorbed at 298 K. Calcined

samples (150 mg) were reduced at 673 K for 1 h in a 60 mL min⁻¹ flow of H₂(5%)/Ar and then cooled down to 298 K. Afterwards, a He stream was bubbled through the solvent in order to saturate the gaseous stream with solvent vapor. Then, the reduced sample was exposed to this stream for 60 min following the effluent composition by mass spectrometry (MS) in a Baltzers Omnistar unit. The weakly adsorbed solvent was removed by flushing with He (60 mL min⁻¹) at 298 K for 1 h. Temperature was then increased at a rate of 10 K min⁻¹ and the composition of the reactor effluent was measured by mass spectrometry.

Calorimetric determinations

Enthalpies of solvent adsorption on Ni/SiO₂ and SiO₂ were experimentally determined by mixing 2 g of sample with 10 mL of each solvent in a calorimeter equipped with a mechanical stirrer and an ERTCO-EUTECHNICS 4400 digital thermometer (0.01 K resolution). In all of the cases, the calorimetric fluid was *n*-dodecane (Sigma, 99%). The catalyst samples were previously reduced and transferred to the calorimeter in conditions similar to those used in the catalytic activity tests. The calorimeter constant was determined by mixing bidistilled water and absolute ethanol (Merck, 99%). The ethanol concentration in the final mixture was 0.05 mol L⁻¹. The corrected temperature increase, due to lack of adiabatic conditions and stirring heat, was calculated by the Dickinson method.²⁷

Catalytic tests

The liquid-phase hydrogenation of butyronitrile (Aldrich, > 99%) was studied at 13 bar (H₂) in a Parr 4843 reactor at 373 K. The autoclave was loaded with 150 mL of solvent, 3 mL of butyronitrile, 1.0 g of catalyst, and 1 mL of *n*-dodecane (Aldrich, > 99%) as internal standard. Toluene (Sigma-Aldrich, 99.8%), ethanol (Cicarelli ACS), benzene (Merck, 99.5%) or cyclohexane (Sigma-Aldrich, 99.5%) were used as solvents. Prior to catalytic tests, samples were reduced *ex situ* in H₂ (60 mL min⁻¹) for 2 h at 673 K and loaded immediately in the reactor at room temperature under inert atmosphere. The reaction system was stirred at 800 rpm and heated to the reaction temperature at 2 K min⁻¹; the H₂ pressure was then rapidly increased to 13 bar.

Product concentrations were followed during the reaction by *ex situ* gas chromatography using an Agilent 6850 GC chromatograph equipped with flame ionization detector, temperature programmer and a 50 m HP-1 capillary column (0.32 mm i.d., 1.05 mm film). Samples from the reaction system were taken by using a loop under pressure in order to avoid flashing. Data were collected every

15-40 min for 450-650 min. The main reaction products detected were BA, DBA, TBA, and BBA. The batch reactor was assumed to be perfectly mixed. Interparticle and intraparticle diffusional limitations were verified as negligible. Conversion of butyronitrile was calculated as $X_{\text{BN}} = C_{\text{BN}} / (C_{\text{BN}}^0 - C_{\text{BN}})$, where C_{BN}^0 is the initial concentration of butyronitrile and C_{BN} is the concentration of butyronitrile at reaction time t . Selectivities (S_j , mol of product j / mol of butyronitrile reacted) were calculated as $S_j = C_j v_{\text{BN}} / (C_{\text{BN}}^0 - C_{\text{BN}}) v_j$ where v_{BN} and v_j are the stoichiometric coefficients of butyronitrile and product j , respectively. Yields (η_j , mol of product j / mol of butyronitrile fed) were calculated as $\eta_j = S_j X_{\text{BN}}$.

Results

Catalyst characterization

The BET surface area of the silica support (300 m² g⁻¹) did not change significantly after metal impregnation and the consecutive oxidation/reduction steps used for obtaining Ni/SiO₂ (290 m² g⁻¹). NiO (ASTM 4-835) was identified from the XRD pattern of calcined Ni/SiO₂ (not shown here). The NiO particle size determined using the Debye-Scherrer equation was 12 nm. The accessible Ni fraction determined by hydrogen chemisorption was low ($D_{\text{Ni}} = 1.0\%$), probably because of the high Ni content.

The NiO/SiO₂ TPR curve was presented in a previous paper.¹¹ Reduction of NiO gave rise to a single TPR peak centered at 643 K which corresponds to the direct reduction of Ni²⁺ ions to Ni⁰.¹² No reduction peaks at higher temperatures that would reveal the presence of less reducible surface Ni silicates were detected.²⁸ From these results, it was inferred that Ni was totally in the metallic state after the standard reduction step used prior to the catalytic tests (reduction in pure H₂ at 673 K).

Solvent properties

Table 1 presents the values of several parameters that define the nature of the solvents used in this work. Specifically, classical polarity parameters (dipole moment μ and dielectric constant ϵ) and other solvatochromic scales (hydrogen-bond donor (α) and hydrogen-bond acceptor (β) parameters, and ET(30) scale) are included in Table 1. Dipole moment μ is a microscopic property, i.e., a property of an individual molecule, while dielectric constant ϵ is a macroscopic property that measures the ability of a bulk material to increase the capacitance of a condenser.²⁹ Solvatochromic parameters α and β are, respectively, related to the electrophilic and nucleophilic properties of a given

compound and measure the solvent ability for hydrogen-bond-donation (HBD) and hydrogen-bond-acceptance (HBA), respectively.³⁰⁻³² Solvatochromic scales of polarity are based on shifts in the absorption spectrum of a reference dye. The position of absorption bands is sensitive to solvent polarity because the electronic distribution of the reference molecule in the excited state is different from that in the ground state. The ET(30) scale is based on the charge-transfer absorption spectra of pyridinium *N*-phenol betaine.²⁹ As the data in Table 1 show, non polar solvents (cyclohexane, toluene and benzene) exhibit low values for ϵ , μ and $E_T(30)$ and they have no capability to act as H-bond donor ($\alpha = 0$). In contrast, protic ethanol has high values for ϵ , μ and $E_T(30)$ and can act as H-bond donor (α value higher than 0.7). The polarity properties of BN and BA are also included in Table 1.

Catalyst activity and selectivity

Figure 1 presents the curves of BN conversion and yields as a function of time obtained for Ni/SiO₂ in ethanol, benzene, toluene and cyclohexane. From the X_{BN} vs. time curves of Figure 1 we determined by polynomial regression and numerical differentiation the initial BN conversion

Table 1. Polarity parameters of BN, BA and the solvents used in this work.^{31,32}

Solvent	ϵ	μ / D	$E_T(30) /$ (kcal mol ⁻¹)	α	β
Ethanol	24.6	1.69	51.9	0.86	0.75
Benzene	2.28	0	34.3	0	0.10
Toluene	2.38	0.37	33.9	0	0.11
Cyclohexane	2.02	0	30.9	0	0
BN	20.3	3.5	42.5	0	0.40
BA	4.92	1.3	37.6	0	0.72

rates *per g* of catalyst (r_{BN}^0 , mmol h⁻¹ g_{cat}⁻¹) that are presented in Table 2. From the r_{BN}^0 values of Table 2 we determined the initial turnover frequencies (TOF, min⁻¹) and the values are included in Table 2. Data for selectivities (S_i) and X_{BN} at the end of the runs are also presented in Table 2.

Regarding catalyst activity, Figure 1 shows that X_{BN} increased continuously on Ni/SiO₂ in all solvents with the progress of the reaction, reaching 100% at the end of the runs. The initial BN conversion rate obtained in different solvents followed the order cyclohexane > ethanol > toluene > benzene (Table 2). The TOF value varied between 63.8 min⁻¹ (cyclohexane) and 19.4 min⁻¹ (benzene). Very few papers have quantitatively determined Ni activity

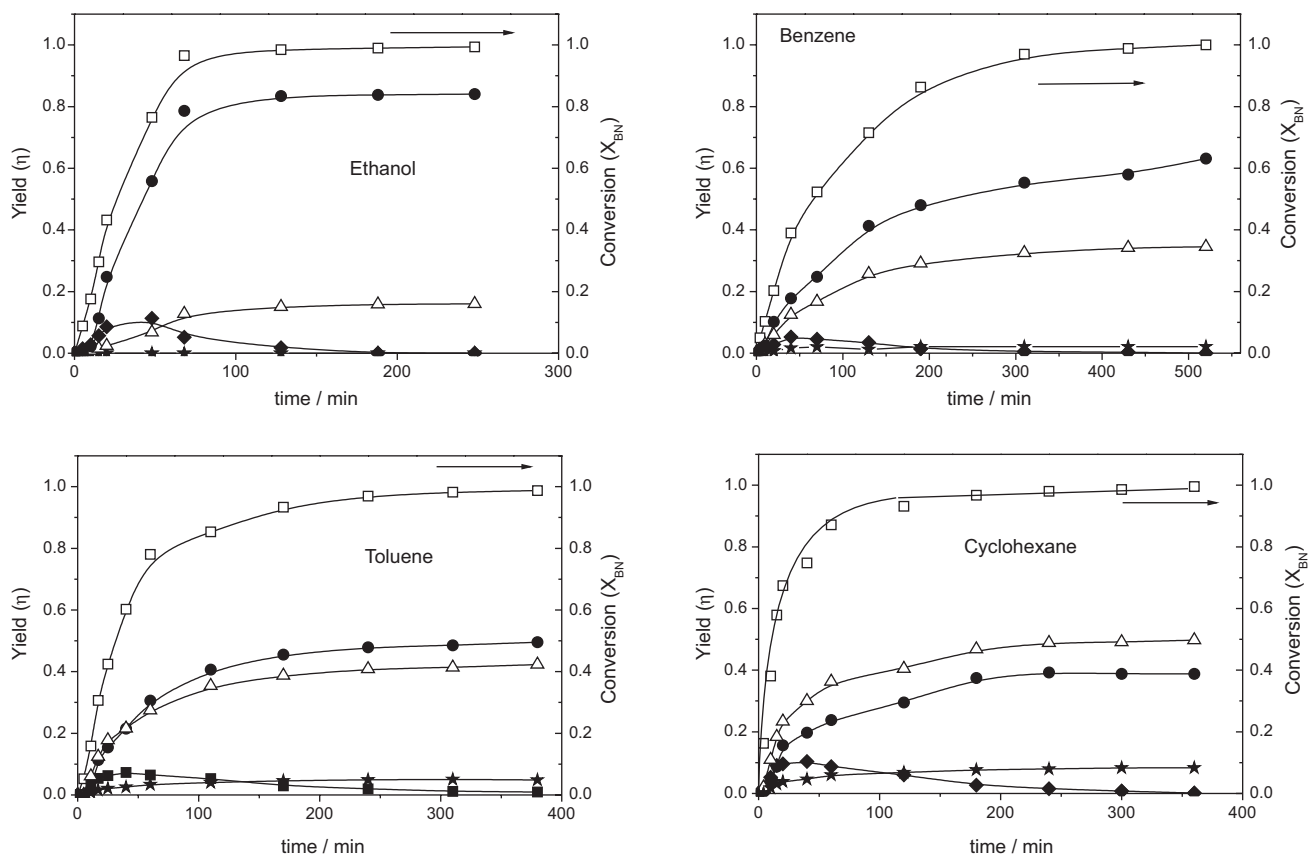


Figure 1. Catalytic results: \square butyronitrile conversion (X_{BN}) and yields (η); \bullet butylamine (BA); \triangle dibutylamine (DBA); \blacklozenge butylidene-butylamine (BBA); \blackstar tributylamine (TBA) [T = 373 K, P = 13 bar, $W_{cat} = 1$ g].

Table 2. Catalytic results

Solvent	Initial activity		Conversion (X_{BN} / %) and selectivities (%) at the end of reaction				
	r_{BN}^0 / (mmol h ⁻¹ g _{cat} ⁻¹)	TOF / min ⁻¹	X_{BN}	BA	DBA	TBA	Others
Ethanol	38.2	35.6	100	84	16	–	–
Benzene	20.8	19.4	100	63	34	2	1
Toluene	29.6	27.6	100	52	43	4	1
Cyclohexane	68.7	63.8	100	39	50	9	2

for the liquid-phase hydrogenation of butyronitrile. Chojceki *et al.*¹⁵ studied this reaction on Raney Ni catalysts at 373 K and 30 bar using octane as solvent and reported a TOF value for BN conversion of 24 min⁻¹ that is comparable with our data in Table 2.

Regarding catalyst selectivity, Ni/SiO₂ in ethanol formed initially BA and BBA. The BA yield increased with the progress of the reaction reaching 84% at the end of the run (Figure 2). The presence of BBA among the reaction products is predicted in the reaction mechanism of Scheme 1 as the Schiff base leading by hydrogenation to the secondary amine. BBA is formed at the beginning of the reaction and then goes through a maximum because it is consecutively hydrogenated to the secondary amine, as depicted in Scheme 1. The local slopes of the η_i curves in Figure 1 give the rate of formation of each product at a specific BN conversion and reaction time. The DBA formation curve in ethanol presents a zero initial slope indicating that DBA is a secondary product as postulated in the reaction network of Scheme 1. At the end of the reaction, Ni/SiO₂ in ethanol yielded a mixture of BA (84%) and DBA (16%), being the carbon balance 100% (Table 2). The Ni/SiO₂ selectivity changed when ethanol was replaced by other solvents. If we consider the sequence ethanol → benzene → toluene → cyclohexane, the data in Table 2 show that the selectivity to BA decreased at the expense of DBA and TBA formation. Thus, the product distribution in cyclohexane was DBA 50%, BA 39% and TBA 9%, being the C balance 98%.

In order to obtain more insight on the effect of solvent on Ni/SiO₂ activity and selectivity we performed additional studies addressing the solvent-Ni interaction strength. Specifically, we determined the solvent adsorption enthalpies on Ni/SiO₂ by calorimetry and we also investigated the temperature-programmed desorption of the solvents on Ni/SiO₂ by analyzing the evolved products by mass spectrometry.

Solvent-catalyst interaction

The results obtained for the TPD of solvents on Ni/SiO₂ are shown in Figure 2. In the case of cyclohexane TPD, we present in Figure 2 the evolution of the m/z 56 signal

(the most intense signal in the cyclohexane fragmentation mass spectrum) and the m/z 28 and 44 signals accounting for possible fragmentation of the cyclohexane molecule. The m/z 2 signal (not shown in Figure 2) was also followed during the TPD of cyclohexane on Ni. Nevertheless, no signals of evolved compounds were detected in the TPD of cyclohexane, thereby showing that cyclohexane was eliminated from the catalyst by the pretreatment with He at 298 K. This result revealed that the interaction between cyclohexane and Ni is very weak.

Desorption of toluene, followed in Figure 2 by the m/z 92 signal corresponding to the molecular ion, occurred at about 350 K. Desorption of several C₂ and C₄ fragments (m/z 28, 43 and 44 signals in Figure 2) formed from toluene-derived species took place at 387 K. These results showed that toluene adsorbs irreversibly on Ni and decomposes at relatively low temperatures. The TPD of benzene was followed by recording the m/z 78 signal that corresponds to the molecular ion, and other signals representing fragments formed from benzene-derived species. In Figure 2 no benzene desorption (m/z 78) was observed while significant evolutions for H₂, C₁ and C₂ species (m/z 2, 16 and 28) were detected at temperatures higher than 500 K. These high-temperature evolutions reflect the decomposition of strongly chemisorbed benzene over Ni. Finally, Figure 2 shows that the desorption temperature maximum of the peaks corresponding to the most abundant ethanol ions (m/z 45, 31, 29, 28 and 27) appeared at 378 K. Two additional broad bands corresponding to high temperature H₂ and C₃ hydrocarbon fragment evolutions (m/z 2 and 44, respectively) were detected between 650 and 820 K. These evolutions indicate the presence of surface nickel sites on which ethanol adsorbs very strongly and decomposes at high temperatures.

The solvent-catalyst interaction strength was also characterized by measuring the average molar adsorption enthalpies (ΔH , kcal mol⁻¹) of the solvents on Ni/SiO₂ by calorimetry. Enthalpy values were estimated by assuming: (i) the total coverage of the metallic surface with a monolayer of the liquid phase species; (ii) the adsorption modes proposed in the literature.³³⁻³⁵ The molar adsorption enthalpies measured on SiO₂ were much lower than those determined

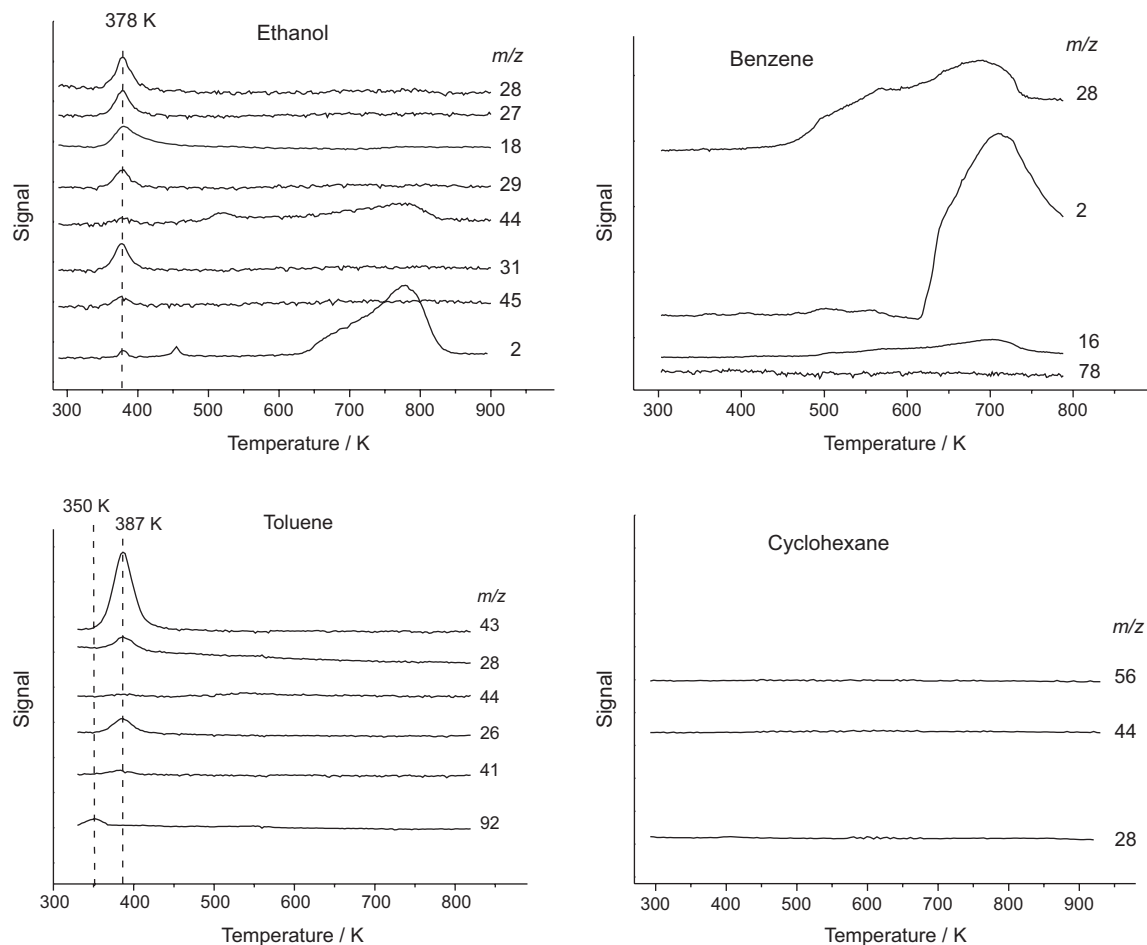


Figure 2. TPD profiles of ethanol, benzene, toluene and cyclohexane preadsorbed at 298 K on Ni/SiO₂ [He stream: 60 mL min⁻¹, heating rate: 10 K min⁻¹].

on Ni/SiO₂ and so they were considered negligible. In the case of non-polar solvents, the average molar adsorption enthalpies determined for benzene, toluene and cyclohexane were 27, 16 and 3 kcal mol⁻¹, respectively. These ΔH values showed that benzene and toluene interact more strongly than cyclohexane with the Ni/SiO₂ surface, which is in agreement with the solvent TPD results of Figure 2. As it has been proposed, the interaction between the cyclohexane saturated ring and metallic Ni surface should be very weak.³⁶ Consistently with our results, previous works have reported that the toluene adsorption on Ni metal is weaker than benzene adsorption, probably because the repulsion forces between the methyl group and metallic nickel surface cause a tilted adsorption of the toluene molecule.^{33,34,37} Finally, we determined that the molar adsorption enthalpy of ethanol on Ni/SiO₂ was about 10 kcal mol⁻¹.

Discussion

Previous reports have stated that the selectivity of metal-supported catalysts for nitrile hydrogenation depends mainly on the metal nature.^{10,11,13} Differences in catalyst selectivity

with the metal nature have been interpreted in terms of the formation of different reactive intermediates and their adsorption strength on the metal surface. In general, it is accepted that on metal catalysts the selective formation of primary amines from nitrile hydrogenation occurs via nitrene intermediates, whereas the preferential formation of secondary and tertiary amines takes place via carbene or aldimine intermediates.^{13,16,38,39} In particular, the preferential formation of BA from BN on Ni, Co, Ru has been attributed to the fact that BN is adsorbed onto the metal via nitrene intermediates.^{40,41} Huang and Sachtler⁴⁰ stated that because the Ru=N bond is very strong the condensation steps yielding secondary and tertiary amines are not favored via “immobile” nitrene intermediates. Similarly, Chojecki *et al.*⁴¹ explained the selective formation of BA from BN on Raney Co and Ni catalysts by speculating that strong binding via the nitrogen atom may stimulate fast hydrogenation of the carbon atom in the nitrile group, which prevents secondary condensation reactions. Here, we observe that Ni/SiO₂ in ethanol, a protic solvent, formed initially BA and then DBA via BBA, but the BA yield at the end of the reaction was very high ($\eta_{BA} = 84\%$), in agreement with previous works

reporting the preferential formation of BA on Ni catalysts. However, Ni activity and selectivity significantly changed when non-polar solvents replaced ethanol; in cyclohexane, Ni/SiO₂ formed preponderantly DBA.

By analyzing the results obtained in non-polar solvents in the sequence benzene → toluene → cyclohexane, it is inferred that the BN conversion rate increases while the selectivity to BA decreases at the expense of DBA and TBA formation. These changes in catalyst activity and selectivity may be explained by considering that the TPD experiment results of Figure 2 and solvent adsorption enthalpies measurements showed that the solvent-metal interaction strength on Ni/SiO₂ follows the order benzene > toluene > cyclohexane. According to the reaction network of Scheme 1, formation of DBA requires the readsorption of BA over the Ni surface to react with butylimine and produce the secondary amine. Thus, selective formation of BA would be favored when a strong solvent-Ni interaction takes place (benzene-Ni interaction, for example) and hinders the readsorption of BA over the metal surface. This assumption explains why the selectivity to DBA increases when benzene is replaced by toluene or cyclohexane, because the reaction between butylimine and adsorbed BA is easier to proceed when the solvent does not compete with both reactants for metal active sites. Similarly, it can be expected that formation of TBA, which is formed by condensation of DBA with butylimine, would be favored in solvents having a weaker interaction with Ni. This is exactly what we observed here because the highest selectivity to TBA was obtained in cyclohexane. This interpretation also explains why the highest BN conversion rate on Ni/SiO₂ was observed in cyclohexane; in fact, because the interaction between cyclohexane and Ni is negligible, the solvent will not block any surface active sites for BN adsorption and conversion.

The highest BA yield on Ni/SiO₂ was obtained in ethanol. This result cannot be explained in terms of stronger ethanol-Ni interaction strength because our results showed that the adsorption enthalpy of ethanol on Ni is lower than those of benzene or toluene. Data in Table 1 shows that ethanol is a protic H-bond donor ($\alpha = 0.86$) solvent that exhibits high values for polarity parameters ϵ , μ and $E_T(30)$. In contrast, BA is an H-bond acceptor molecule of $\beta = 0.72$. Thus, it can be expected that a strong interaction will exist between BA and protic ethanol causing BA solvation in the liquid phase. The BA molecules would be then surrounded by alcohol molecules that would hinder BA adsorption on Ni and, as a consequence, also the formation of DBA that occurs by surface condensation between BA and butylimine. The solvation of BA in ethanol, i.e., a solvent-reactant

interaction, would explain then the high selectivity to BA that Ni/SiO₂ exhibits in this alcohol.

In summary, if the butyronitrile hydrogenation reaction is performed in non-polar solvents, selective BA formation is favored when a strong solvent-Ni interaction takes place and hinders the readsorption of BA over the metal surface. Nevertheless, the highest BA yields are obtained in protic alcohols, such as ethanol, that strongly interact with BA in the liquid phase and hamper BA adsorption on the catalyst.

Conclusions

Solvent nature plays a crucial role in controlling the Ni/SiO₂ activity and selectivity for the synthesis of *n*-butylamine from butyronitrile hydrogenation. When non-polar solvents such as cyclohexane, toluene or benzene are used, the solvent-catalyst interaction strength determines the selectivity to *n*-butylamine: the stronger the solvent-catalyst interaction the higher the *n*-butylamine yield. This is because a strong solvent-Ni interaction hinders the readsorption of *n*-butylamine over the metal surface and, as a consequence, impedes the formation of dibutylamine that occurs by surface condensation between *n*-butylamine and butylimine.

If the reaction is carried out in protic alcohols, such as ethanol, the solvent-butylamine interaction strength in the liquid phase controls the selectivity to *n*-butylamine on Ni/SiO₂. Ethanol is an H-bond donor solvent that strongly interacts with H-bond acceptor *n*-butylamine and causes its solvation in the liquid phase. The *n*-butylamine molecules are then surrounded by alcohol molecules that hinder *n*-butylamine adsorption on Ni and, as a consequence, also decrease the consecutive formation of dibutylamine.

Acknowledgements

We thank the Universidad Nacional del Litoral (UNL), the Agencia Nacional de Promoción Científica y Tecnológica (ANPCyT) and the Consejo Nacional de Investigaciones Científicas y Técnicas (CONICET), Argentina, for the financial support of this work.

References

1. Turcotte, M. G.; Johnson, T. A. In *Kirk-Othmer Encyclopedia of Chemical Technology*; Kroschwitz, J. I., ed.; Wiley: New York, 1992, pp. 369.
2. Kukula, P.; Studer, M.; Blaser, H. U.; *Adv. Synth. Catal.* **2004**, *346*, 1487.
3. Das, S.; Zhou, S.; Addis, D.; Enthaler, S.; Junge, K.; Beller, M.; *Top. Catal.* **2010**, *53*, 979.

4. Sabatier, P.; Senderens, J. B.; *C. R. Hebd. Seances Acad. Sci.* **1905**, *140*, 482.
5. Von Braun, J.; Blessing, G.; Zobel, F.; *Ber. Dtsch. Chem. Ges.* **1923**, *36*, 1988.
6. Juday, R.; Adkins, H.; *J. Am. Chem. Soc.* **1955**, *77*, 4559.
7. Greenfield, H.; *I&EC Prod. Res. Dev.* **1967**, *6*, 142.
8. Witte, P. T.; *Collect. Czech. Chem. Commun.* **2007**, *72*, 468.
9. Ortiz-Hernandez, I.; Williams, C. T.; *Langmuir* **2007**, *23*, 3172.
10. Huang, Y.; Sachtler, W. M. H.; *Appl. Catal., A* **1999**, *182*, 365.
11. Segobia, D. J.; Trasarti, A. F.; Apesteguía, C. R.; *Appl. Catal., A* **2012**, *445-446*, 69.
12. Volf, J.; Pasek, J.; *Stud. Surf. Sci. Catal.* **1986**, *27*, 105.
13. Krupka, J.; Pasek, J.; *Curr. Org. Chem.* **2012**, *16*, 988.
14. Hochard, F.; Jobic, H.; Massardier, J.; Renouprez, A. J.; *J. Mol. Catal. A: Chem.* **1995**, *95*, 163.
15. Chojecki, A.; Veprek-Hejman, M.; Müller, T. E.; Schäringer, P.; Veprek, S.; Lercher, J. A.; *J. Catal.* **2007**, *245*, 237.
16. Schäringer, P.; Müller, T. E.; Jentys, A.; Lercher, J. A.; *J. Catal.* **2009**, *263*, 34.
17. Huang, Y.; Adeeva, V.; Sachtler, W. M. H.; *Appl. Catal., A* **2000**, *196*, 73.
18. Li, H.; Wu, Y.; Luo, H.; Wang, M.; Xu, Y.; *J. Catal.* **2003**, *214*, 15.
19. Yadav, G. D.; Kharkara, M. R.; *Appl. Catal., A* **1995**, *126*, 115.
20. Rylander, P. N.; *Catalytic Hydrogenation over Platinum Metals*; Academic Press: New York, 1967.
21. Hegedus, L.; Máthé, T.; Kárpáti, T.; *Appl. Catal., A* **2008**, *349*, 40.
22. Besson, M.; Bonnier, J. M.; Joucla, M.; *Bull. Soc. Chim. Fr.* **1990**, *127*, 5.
23. Bertero, N. M.; Apesteguía, C. R.; Marchi, A. J.; *Appl. Catal., A* **2008**, *349*, 100.
24. Bertero, N. M.; Trasarti, A. F.; Apesteguía, C. R.; Marchi, A. J.; *Appl. Catal., A* **2011**, *394*, 228.
25. Bertero, N. M.; Trasarti, A. F.; Apesteguía, C. R.; Marchi, A. J.; *Appl. Catal., A* **2014**, *475*, 282.
26. Borgna, A.; Garetto, T. F.; Apesteguía, C. R.; Le Normand, F.; Moraweck, B.; *J. Catal.* **1999**, *186*, 433.
27. Coops, J.; Jessup, R. S.; van Nes, K. In *Experimental Thermochemistry*; Rossini, F. D., ed.; Interscience: New York, 1956, pp. 6.
28. Trasarti, A. F.; Marchi, A. J.; Apesteguía, C. R.; *Catal. Comm.* **2013**, *32*, 62.
29. Reidhardt, C.; *Solvents and Solvent Effects in Organic Chemistry*; Wiley VCH: New York, 2004.
30. Kamlet, M. J.; Abboud, J. L. M.; Abraham, M. H.; Grellier, P. L.; Doherty, R. M.; Taft, R.; *Can. J. Chem.* **1988**, *66*, 2673.
31. Marcus, Y.; *Chem. Soc. Rev.* **1993**, *22*, 409.
32. Reichardt, C.; *Chem. Rev.* **1994**, *94*, 2319.
33. Friend, C. M.; Muetterties, E. L.; *J. Am. Chem. Soc.* **1981**, *103*, 773.
34. Myers, A. K.; Schoofs, G. R.; Benziger, J. B.; *J. Phys. Chem.* **1987**, *91*, 2230.
35. Bigot, B.; Delbecq, F.; Milet, A.; Peuch, V.; *J. Catal.* **1996**, *159*, 383.
36. Rautanen, P. A.; Aittamaa, J. R.; Krause, A. O. I.; *Ind. Eng. Chem. Res.* **2000**, *39*, 4032.
37. Myers, A. K.; Benziger, J. B.; *Langmuir* **1987**, *3*, 414.
38. Coq, B.; Tichit, D.; Ribet, S.; *J. Catal.* **2000**, *189*, 117.
39. Poupin, C.; Maache, R.; Pirault-Roy, L.; Brahmi, R.; Williams, C. T.; *Appl. Catal., A* **2014**, *475*, 363.
40. Huang, J. Y.; Sachtler, W. M. H.; *J. Catal.* **1999**, *184*, 247.
41. Chojecki, A.; Jobic, H.; Jentys, A.; Müller, T. E.; Lercher, J. A.; *Catal. Lett.* **2004**, *7*, 155.

Submitted: June 26, 2014

Published online: September 16, 2014